THE JOURNAL OF BIOLOGICAL CHEMISTRY VOL. 291, NO. 28, pp. 14609–14619, July 8, 2016

Substrate Specificity of Purified Recombinant Chicken β-Carotene 9′,10′-Oxygenase (BCO2)*

Received for publication, February 23, 2016, and in revised form, April 27, 2016 Published, JBC Papers in Press, May 3, 2016, DOI 10.1074/jbc.M116.723684

Carlo dela Seña[‡§], Jian Sun[‡], Sureshbabu Narayanasamy[‡], Kenneth M. Riedl[¶], Yan Yuan[‡], Robert W. Curley, Jr.[§‖], Steven J. Schwartz[¶], and Earl H. Harrison[‡§1]

From the [‡]Department of Human Nutrition, [§]Ohio State Biochemistry Program, [¶]Department of Food Science and Technology, and [‖]College of Pharmacy, The Ohio State University, Columbus, Ohio 43210

Provitamin A carotenoids are oxidatively cleaved by β-carotene 15,15′-dioxygenase (BCO1) at the central 15-15′ double bond to form retinal (vitamin A aldehyde). Another carotenoid oxygenase, β-carotene 9′,10′-oxygenase (BCO2) catalyzes the oxidative cleavage of carotenoids at the 9′-10′ bond to yield an ionone and an apo-10′-carotenoid. Previously published substrate specificity studies of BCO2 were conducted using crude lysates from bacteria or insect cells expressing recombinant BCO2. Our attempts to obtain active recombinant human BCO2 expressed in *Escherichia coli* were unsuccessful. We have expressed recombinant chicken BCO2 in the strain *E. coli* BL21-Gold (DE3) and purified the enzyme by cobalt ion affinity chromatography. Like BCO1, purified recombinant chicken BCO2 catalyzes the oxidative cleavage of the provitamin A carotenoids β-carotene, α-carotene, and β-cryptoxanthin. Its catalytic activity with β-carotene as substrate is at least 10-fold lower than that of BCO1. In further contrast to BCO1, purified recombinant chicken BCO2 also catalyzes the oxidative cleavage of 9-*cis*-β-carotene and the non-provitamin A carotenoids zeaxanthin and lutein, and is inactive with all-*trans*-lycopene and β-apocarotenoids. Apo-10′-carotenoids were detected as enzymatic products by HPLC, and the identities were confirmed by LC-MS. Small amounts of 3-hydroxy-β-apo-8′-carotenal were also consistently detected in BCO2-β-cryptoxanthin reaction mixtures. With the exception of this activity with β-cryptoxanthin, BCO2 cleaves specifically at the 9′-10′ bond to produce apo-10′-carotenoids. BCO2 has been shown to function in preventing the excessive accumulation of carotenoids, and its broad substrate specificity is consistent with this.

There are three members of the carotenoid oxygenase family expressed in vertebrates. β-Carotene 15,15′-dioxygenase (BCO1)[2] catalyzes the oxidative cleavage of provitamin A carotenoids to form retinal (vitamin A aldehyde). RPE65 is an isomerohydrolase that catalyzes the conversion of all-*trans*-retinyl esters to 11-*cis*-retinol and is an important component of the visual cycle (1–5). β-Carotene 9′,10′-oxygenase (BCO2) catalyzes the oxidative cleavage of carotenoids at the 9′-10′ or 9-10 bond to yield an ionone and an apo-10′-carotenoid. Studies in mice suggest that BCO2 cleavage prevents oxidative stress from carotenoid accumulation, especially in the mitochondria (6). The provitamin A carotenoids β-carotene and β-cryptoxanthin are also cleaved by BCO2 to produce β-apo-10′-carotenal (6–8), which can then be oxidatively cleaved by BCO1 to produce retinal (8, 9).

Unlike BCO1, BCO2 has also been shown to cleave non-provitamin A carotenoids such as zeaxanthin and lutein to produce 3-hydroxy-apo-10′-carotenals (6, 7). The significance of these compounds in mammals is unknown. However, (3*R*)-hydroxy-β-apo-10′-carotenol, also known as galloxanthin, has been identified as one of the dominant carotenoids in quail retina (10). This is formed from the reduction of (3*R*)-hydroxy-β-apo-10′-carotenal, which can be formed from BCO2 cleavage of β-cryptoxanthin, zeaxanthin, or lutein. Galloxanthin is found in the lipid droplets of avian cones that is necessary for the filtering of the short wavelength UV light in the avian eye. This process is evolutionarily important for the enhanced color vision of birds as compared with other taxa. Ferret hepatic homogenates have been shown to reduce (3*R*)-hydroxy-β-apo-10′-carotenal to the alcohol (7). The production of β-apo-10′-carotenol has been shown *in vivo*. BCO1 KO mice, which have elevated expression of BCO2, accumulate β-apo-10′-carotenol on a diet with only β-carotene as the sole source of apocarotenoids (11). In humans, the dominant carotenoids in the retina are lutein, 3′-epilutein, and zeaxanthin (10). Given that BCO2 is also highly expressed in the human retinal epithelium (12), it is interesting that BCO2 cleavage products of xanthophylls are not the dominant carotenoids. It is possible that human BCO2 and avian BCO2 have different substrate specificities, or another regulatory mechanism(s) exists to favor the BCO2 cleavage of lutein and zeaxanthin in avian retina but not in humans (13, 14). There are currently five isoforms of human BCO2 described in the National Center for Biotechnology Information (NCBI) Database (see Fig. 1). It is also possible that the inactive isoform is expressed in the human retinal pigment epithelium.

The published BCO2 substrate specificity studies as of the time of writing were done with crude lysates of bacteria and insects cells expressing recombinant BCO2 (6, 7, 14). In this work, we describe the substrate specificity and kinetics of β-carotene cleavage of purified recombinant chicken BCO2. We show that the enzyme reacts with β-carotene (albeit with

* This work was supported by National Institutes of Health Grant R01-HL49879 and a grant from the Ohio Agricultural Research Development Center. The authors declare that they have no conflicts of interest with the contents of this article. The content is solely the responsibility of the authors and does not necessarily represent the official views of the National Institutes of Health.

[1] To whom correspondence should be addressed: Ohio State University, 314 Campbell Hall, 1787 Neil Ave., Columbus, OH 43210. Tel.: 614-292-8189; Fax: 614-292-8880; E-mail: harrison.304@osu.edu.

[2] The abbreviations used are: BCO1, β-carotene 15,15′-oxygenase; BCO2, β-carotene 9′,10′-oxygenase; Tricine, *N*-[2-hydroxy-1,1-bis(hydroxymethyl)ethyl]glycine; Q-TOF, quadrupole time-of-flight.

lower activity than BCO1) and with α-carotene, β-cryptoxanthin, zeaxanthin, and lutein but not with lycopene and β-apocarotenals.

Experimental Procedures

Carotenoids and Retinoids

Unless indicated, all carotenoids and apocarotenoids are the all-*trans* form. β-Carotene (≥97%), retinal (≥98%), and β-apo-8′-carotenal (≥96%) were purchased from Sigma-Aldrich. α-Carotene (≥95%) and β-cryptoxanthin (≥97% were purchased from Santa Cruz Biotechnology. Zeaxanthin (≥98%) and lutein (≥93%) were purchased from Indofine Chemical Co. The lycopene standard (92% all-*trans*, 6% 5-*cis*, 2% other isomers) was prepared by extraction from tomato paste and crystallization. β-Apo-10′-carotenal, β-apo-12′-carotenal, and β-apo-14′-carotenal were synthesized according to published methods (15). The purification of 9-*cis*-β-carotene from Betatene® is described in our previous publication (9).

Plasmids

Plasmids for bacterial expression containing human BCO2 isoforms *a* and *d* with a C-terminal His tag were purchased from GeneCopoeia. A pET-28a plasmid vector containing the cDNA of chicken BCO2 with an N-terminal hexahistidine tag was a gift from Drs. Matthew Toomey and Joseph Corbo of Washington University at St. Louis.

Expression and Purification of Recombinant BCO2

For human BCO2 isoforms *a* and *d*, the plasmid was transformed into *E. coli* BL21-Gold (DE3) (Stratagene) or T7 Express (New England Biolabs) according to the manufacturer's instructions. For chicken BCO2, the plasmid was transformed into *E. coli* BL21-Gold (DE3). The transformed bacterial cells were grown in LB broth (Sigma-Aldrich) at 30 °C to an A_{600} of 0.5–0.7. The incubator temperature was then lowered to 16 °C, and expression of the recombinant protein was induced by adding isopropyl 1-thio-β-D-galactopyranoside (Gold Biotechnology) to a final concentration of 0.1 mM. Five liters of culture were grown for 16 h, and the cells were harvested by centrifugation. The cell pastes were frozen at −80 °C and thawed prior to lysis. The protein was purified using the same protocol for recombinant human BCO1 using cobalt ion affinity chromatography as in our previous publication (9).

In Vitro BCO2 Assay

The *in vitro* BCO2 enzyme assay was based on the method of Amengual *et al.* (6). All substrates were tested at a concentration of 20 μM at 37 °C with the indicated incubation time and protein concentration. The working enzyme solution for a single reaction was prepared by combining the required amount of enzyme and storage buffer to a total volume of 100 μl, 40 μl of reaction buffer (250 mM Tricine-KOH, pH 8.0 at 37 °C, 625 mM NaCl), 4 μl of 500 μM $FeSO_4$, 2 μl of 0.5 M tris(2-carboxyethyl)phosphine, and 14 μl of deionized water. The substrate solution was prepared by first mixing the required amount of carotenoid in hexanes or ethanol, 9 μl of 10 mM α-tocopherol, 225 μl of 4% octyl thioglucoside in ethanol, and 400 μl of acetone. The mixture was dried under nitrogen and stored at −20 °C. The next day, immediately before use, the residue was brought up to ice bath temperature, redissolved in 200 μl of acetone, dried down under nitrogen, and redissolved in 180 μl of deionized water. The substrate and enzyme solutions were incubated at 37 °C for 5 min, and the reaction was initiated by adding 40 μl of the substrate to the enzyme for a total reaction volume of 200 μl. The reaction was quenched with 50 μl of 37% formaldehyde and incubated for a further 10 min at 37 °C. Then 500 μl of 1:1 (v/v) acetonitrile-isopropyl alcohol was added. The resulting mixture was filtered through a 0.22-μm syringe filter, and 100 μl was subjected to HPLC. Time 0, no enzyme, and heat-denatured enzyme controls were used.

Analytical HPLC Methods

Method A—This is identical to Method A as described in our previous publication (9) using a Zorbax Eclipse XDB-C_{18} LC column (4.6 × 50 mm, 1.8 μm; Agilent) with or without a Zorbax Eclipse XDB-C_{18} guard column (4.6 × 12.5 mm, 5 μm; Agilent).

Method B—For lutein, the chromatography described above cannot separate the 3-hydroxy-β-apo-10′-carotenal and 3-hydroxy-α-apo-10′-carotenal produced from its reaction with BCO2. However, these were separated by the following chromatography system: column, YMC Carotenoid (YMC Co.), 4.6 × 150 mm, 5-μm particle size; flow rate, 0.9 ml/min; column temperature, 35 °C; solvent, 95% methanol: 5% water; elution time, 12 min. Elution was monitored at 380, 414, and 453 nm.

Method C—The reaction products and isomers of the parent carotenoids were analyzed using a YMC Carotenoid S-3 column (4.6 × 250 mm, 3-μm particle size), a flow rate of 1.4 ml/min, and a column temperature of 35 °C. The following elution profile was used with methanol (solvent A) and methyl *tert*-butyl ether (solvent B): gradient from 5 to 25% B over 30 min, gradient from 25 to 5% solvent B over 30 s, and 5% solvent B for 2.5 min. Elution was monitored at 450 and 360 nm.

LC-MS Analysis

HPLC was performed with Method A described above with the following modifications. First, formic acid was used instead of ammonium acetate. Second, the column used was also Zorbax XDB-C_{18} but with dimensions of 4.6 × 150 mm and 5-μm particle size.

The HPLC was interfaced with a quadrupole time-of-flight (Q-TOF) mass spectrometer (Q-TOF Premier, Micromass, Manchester, UK) via an atmospheric pressure chemical ionization probe. β-Carotene, β-apo-8′-carotenal, β-apo-10′-carotenal, β-apo-12′-carotenal, β-apo-14′-carotenal, and retinal were ionized in atmospheric pressure chemical ionization negative mode as their respective radical anions, 536.438, 416.310, 376.280, 350.260, 310.230, and 284.210 *m*/*z*. The Q-TOF system allowed for quantitative detection with the confidence of accurate mass typically being 1 ppm. Mass spectra were acquired in V-mode (~8000 resolution) from 50 to 1000 *m*/*z* with a scan time of 1 s, peak centroiding, and enhanced duty cycle enabled for the parent *m*/*z*. At intervals of 30 s, a 0.1-s lock spray scan was acquired with leucine enkephalin as the lock spray compound (554.2615 *m*/*z*) to correct for minor deviations in calibration due to temperature fluctuations. Prior to

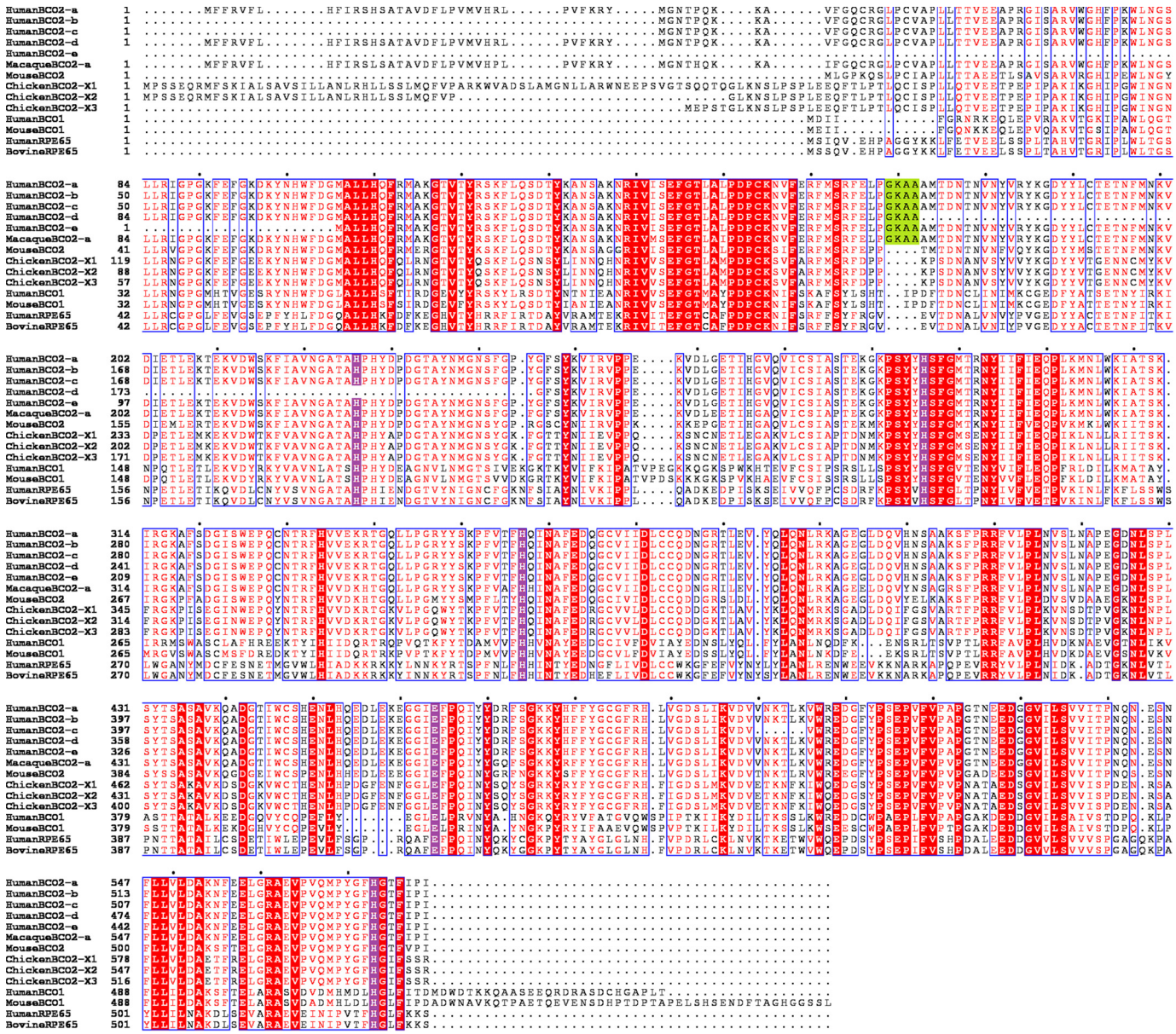

FIGURE 1. **Sequence alignment of BCO2, BCO1, and RPE65.** The GKAA insertion that differentiates human BCO2 isoforms from other BCO2 orthologs is highlighted in *green*. The conserved residues (four histidines and one glutamate) that were identified to be crucial for activity in mouse BCO1 (17) are highlighted in *violet*. The sequence alignment was generated by ClustalW (37), and the image was generated by ESPript (38) (*green* and *violet* highlights were added separately). The NCBI accession numbers are as follows: human BCO2 isoforms *a–e*, NP_114144.4, NP_001032367.2, NP_001243326.1, NP_001243327.1, and NP_001243329.1, respectively; macaque BCO2, AFE80390.1; mouse BCO2, NP_573480.1; chicken BCO2 isoforms *x1–x3*, XP_004948199.1, XP_417929.2, and XP_015153786.1, respectively; human BCO1, NP_059125.2; mouse BCO1, NP_067461.2; human RPE65, NP_000320.1; bovine RPE65, NP_776878.1. The *dots* are space markers for 10 amino acids of the topmost sequence.

analysis, the Q-TOF was fully calibrated from 114 to 1473 m/z using a solution of sodium formate. The resultant MS spectra were acquired and integrated with MassLynx software, V4.1 (Micromass). Source parameters were as follows: 30-μA corona current; 550 °C probe; 110 °C source block; 35-V cone; 100 liter/h cone gas (N_2); 400 liter/h desolvation gas (N_2); and collision energy of 8 eV (non-fragmenting) with argon as the collision-induced dissociation gas (4.2×10^{-3} millibar).

Results

Recombinant Human BCO2 Expressed in E. coli Is Inactive—The longest isoform of human BCO2 is isoform *a* (accession number NP_114144.4), corresponding to a 579-amino acid peptide. Isoform *d* (accession number NP_001243327.1) corresponds to a 506-amino acid peptide and is the same sequence used by Kim *et al.* (16) in their study claiming to produce active recombinant human BCO2 in *E. coli*. strain ER2566 (equivalent to T7 Express). Interestingly, this isoform is missing one of the conserved histidines that coordinate the catalytic ferrous ion (Fig. 1) (17).

Both isoforms have a behavior similar to that of recombinant human BCO1 expressed in *E. coli* (9): high rates of expression favor formation of inclusion bodies, but the small amount of His-tagged protein can be recovered from the supernatant by cobalt ion affinity chromatography. However, there is no detectable enzymatic cleavage activity from the crude superna-

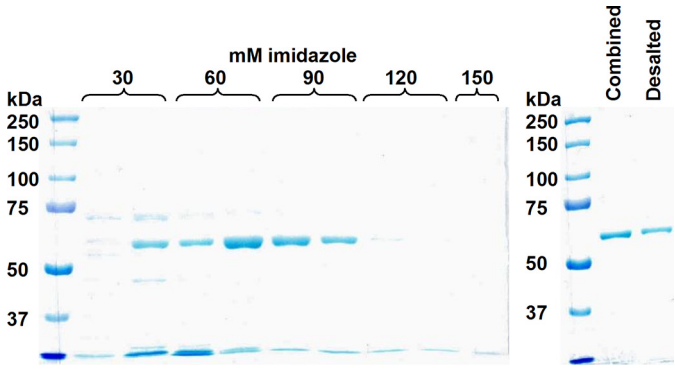

FIGURE 2. **Purification of recombinant chicken BCO2 using cobalt affinity column chromatography.** The SDS-polyacrylamide gel on the *left* shows the elution of recombinant His-tagged human BCO2 (theoretical mass, 64,202 Da) from the cobalt column by increasing concentrations of imidazole. Only the fractions that show a single band (*lanes 5–7*) were combined and desalted into the final storage buffer. The SDS-polyacrylamide gel on the *right* shows the combined fractions and the protein obtained after desalting.

tant and the purified protein from either strain of *E. coli* when tested with β-carotene, β-cryptoxanthin, and lutein. Furthermore, we did not detect any activity when the *in vitro* assay was conducted in the same manner as BCO1 (9) or by the method of Amengual *et al.* (6). The inactivity of recombinant human BCO2 expressed in *E. coli* has been reported by others (13, 14).

Expression and Purification of Recombinant Chicken BCO2—The pET28a-chicken BCO2 clone is similar to isoform *x2* of *Gallus gallus* BCO2 mRNA in PubMed (accession number XP_417929.2; corresponding to a 579-amino acid peptide), but the first 31 amino acids of the latter (MPSSEQRMFSKIALSAVSILLANLRHLLSSL) are replaced with 16 amino acids (MGSSHHHHHHSSGLVPRGSH) corresponding to the His tag. The theoretical molecular mass of the protein is 64,202 Da. As with recombinant human BCO2 and BCO1, recombinant chicken BCO2 is not very soluble under the expression conditions in BL21-Gold (DE3), but the small amount of soluble protein was easily recovered to a high degree of purity by cobalt ion affinity chromatography as shown in Fig. 2.

Kinetics of Cleavage of β-Carotene by Chicken BCO2—Kinetic data for the cleavage of all-*trans*-β-carotene by purified recombinant chicken BCO2 is shown in Fig. 3. The production of β-apo-10′-carotenal is linear for up to 40 min (Fig. 3*A*) and up to 5 μg of BCO2/200-μl reaction (Fig. 3*B*). The substrate-velocity curve (Fig. 3*C*) fits the Michaelis-Menten equation with a V_{max} of 0.93 nmol of β-apo-10′-carotenal/mg of BCO2/h (standard error of regression, 0.05; two independent experiments) and K_m of 2.03 μM (standard error of regression, 0.27; two independent experiments) obtained from nonlinear regression using GraphPad Prism 4. From these values, the calculated k_{cat} is 9.9×10^{-4} min^{-1}, and k_{cat}/K_m (catalytic efficiency) is 487 M^{-1} min^{-1}. This catalytic efficiency is at least 10 times lower than what we have previously measured for purified recombinant human BCO1 (6098 M^{-1} min^{-1}) (9).

Chicken BCO2 Cleaves Full-length β-Ring Carotenoids at the 9′-10′ Bond—The activity of purified recombinant chicken BCO2 was tested with the major dietary carotenoids (all-*trans*-β-carotene, 9-*cis*-β-carotene, α-carotene, β-cryptoxanthin, zeaxanthin, lutein, and lycopene) and β-apocarotenals (β-apo-8′-carotenal, β-apo-10′-carotenal, β-apo-12′-carotenal, and β-apo-14′-carotenal) using a 20 μM concentration of each substrate and 10 μg of BCO2/200-μl reaction with a 2-h reaction time. Time 0, no enzyme, and heat-denatured enzyme controls were conducted for all reactions.

Because 9-*cis*-β-carotene is an asymmetrical molecule, we expected to see two apocarotenoid cleavage products, all-*trans*- and 9-*cis*-β-apo-10′-carotenal (Fig. 4). In our original chromatography (HPLC Method A), there was only one enzymatic product peak observed from all-*trans*- and 9-*cis*-β-carotene, and these have the same retention time as standard all-*trans*-β-apo-10′-carotenal (Fig. 5, *A–C*). However, when using a different chromatographic system (HPLC Method C), the cleavage product of 9-*cis*-β-carotene elutes earlier (about 0.1 min) than the cleavage product of all-*trans*-β-carotene and standard all-*trans*-β-apo-10′-carotenal (Fig. 5*D*). The peak of the cleavage product of 9-*cis*-β-carotene shows a very small shoulder to the right. However, the heat-denatured control shows that there is a distorted peak at that elution time. Thus, we cannot rule out the possibility that some all-*trans*-β-apo-10′-carotenal is also produced by enzymatic cleavage. Nevertheless, it is quite clear that the cleavage product of 9-*cis*-β-carotene is *not* solely all-*trans*-β-apo-10′-carotenal. It is also worth noting that we cannot detect any conversion of the parent 9-*cis*-β-carotene to the all-*trans* form (and vice versa) during the reaction (Fig. 5*E*). Thus, the major (if not the only) product of BCO2 cleavage of 9-*cis*-β-carotene under the test conditions is 9-*cis*-β-apo-10′-carotenal.

α-Carotene is an asymmetrical molecule, and BCO2 cleavage can produce two products, β-apo-10′-carotenal and α-apo-10′-carotenal (Fig. 6). Consequently, we observed two product peaks (Fig. 7*A*), one with the same retention time as β-apo-8′-carotenal (peak *b*) and another earlier eluting peak that corresponds to α-apo-8′-carotenal (peak *a*).

β-Cryptoxanthin is also an asymmetrical molecule, and BCO2 cleavage can produce two products, β-apo-10′-carotenal and 3-hydroxy-β-apo-10′-carotenal (Fig. 6). We observed three product peaks (Fig. 7*B*). β-Apo-10′-carotenal (peak *e*) was identified by its identical retention time to the standard compound and LC-MS, and 3-hydroxy-β-apo-10′-carotenal (peak *c*) was identified by LC-MS. 3-Hydroxy-β-apo-8′-carotenal, a product of 7-8 double bond cleavage, was identified by LC-MS (peak *d*). Note that because of the response range used in the figure, this peak appears small, but its height is comparable with that of the product peak for all-*trans* β-carotene (Fig. 5*A*). The UV-visible spectra of peak *d* is also consistent with 3-hydroxy-β-apo-8′-carotenal. The chromophore of carotenoids and apocarotenoids is the conjugated double bond system, and hydroxylation that does not disrupt the latter does not cause large shifts in λ_{max} (18). Thus, the UV spectra of 3-hydroxy-β-apo-10′-carotenal and β-apo-10′-carotenal produced from the reaction and that of standard β-apo-10′-carotenal show the same λ_{max} (Fig. 8, *left column*). However, the UV spectrum of peak *d* is more similar to that of standard β-apo-8′-carotenal rather than that of β-apo-10′-carotenal (Fig. 8, *right column*).

A substrate-velocity curve was done for β-cryptoxanthin (Fig. 9). However, apart from β-apo-10′-carotenal and β-apo-8′-carotenal, we do not have authentic standards for other apocarotenal cleavage products necessary for their quantification.

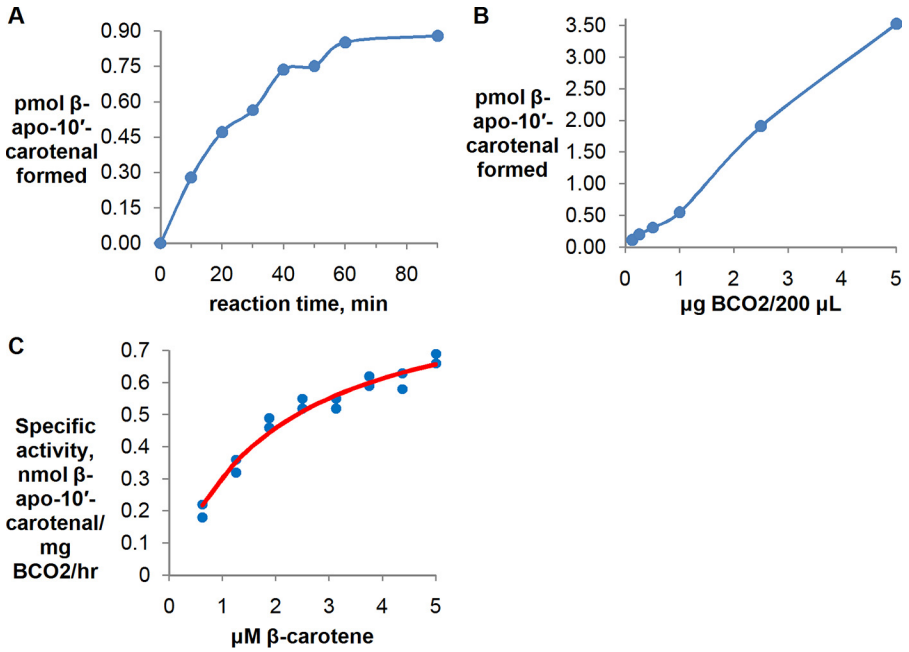

FIGURE 3. **Kinetic data for purified recombinant chicken BCO2 with β-carotene at 37 °C.** Each data point represents the difference between the average of duplicate measurements at a given reaction time and the average of duplicate time 0 controls. *A*, time course using 5 μM β-carotene incubated with 1000 ng of BCO2. *B*, protein curve using 5 μM β-carotene and a 30-min reaction time. *C*, plot of reaction velocity as a function of β-carotene concentration using 1 μg of BCO2/200-μl reaction and a 30-min reaction time. The results of two independent experiments (two different preparations of purified protein) are shown and fit to the Michaelis-Menten equation. The *red* trace is the best fitting Michaelis-Menten curve generated by GraphPad Prism 4.

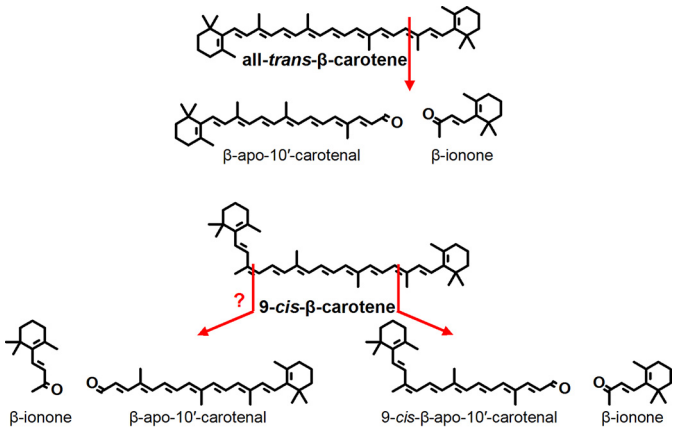

FIGURE 4. **Structures of the 9-10 and 9′-10′ cleavage of all-*trans*- and 9-*cis*-β-carotene.** The production of all-*trans*-β-apo-10′-carotenal from 9-*cis*-β-carotene has not been completely resolved by this study.

Thus, the 3-hydroxy-β-apocarotenal product peaks were estimated by using the analogous β-apocarotenals. Even though the hydroxyl group is not expected to cause large changes in λ_{max} and extinction coefficients for as long as the conjugated system is not disrupted (18), we cannot guarantee that the instrument response is virtually the same. Thus, kinetic parameters cannot be reliably calculated. Even if the standards were available, the data cannot be fit to the classic Michaelis-Menten model because the enzyme cleaves the substrate at three positions, and each position is presumably a separate binding mode.

Zeaxanthin is a symmetrical molecule, and BCO2 cleavage will yield 3-hydroxy-β-apo-10′-carotenal (Fig. 6). Consequently, we also observed a product peak (Fig. 7*C*, peak *f*) with the same retention time as peak *c* for β-cryptoxanthin (Fig. 7*B*).

Lutein is another asymmetrical substrate that can yield two apocarotenoids products, 3-hydroxy-β-apo-10′-carotenal and 3-hydroxy-α-apo-10′-carotenal (Fig. 6). The original chromatography used (HPLC Method A) shows only one product peak (Fig. 7*D*, peak *g*). However, HPLC Method B was able to separate the two products (Fig. 10, *top panel*). 3-Hydroxy-β-apo-10′-carotenal was distinguished from the α isomer by its identical retention time to the 3-hydroxy-β-apo-10′-carotenal produced from BCO2 cleavage of zeaxanthin (Fig. 10, *bottom panel*).

It has been reported that murine BCO2 can cleave the two ionone rings from the carotenoid to yield rosafluene dialdehyde (6). However, by identification of the masses of the cleavage products by LC-MS, we did not find evidence of its formation even with a 2-h reaction time and 25 μg of protein/200-μl reaction. Also, incubation of β-apo-10′-carotenal with chicken BCO2 did not show any evidence of a reaction. We also did not detect any reaction between chicken BCO2 and β-apo-8′-carotenal, β-apo-12′-carotenal, β-apo-14′-carotenal, and lycopene (chemical structures shown in Fig. 11).

Discussion

Products of excentric cleavage of carotenoids are important in the production of plant hormones such as abscisic acid and strigolactone (19). For vertebrates, the central cleavage product of provitamin A carotenoids, retinal, is still the most important in terms of function. Our finding that the central bond cleavage enzyme BCO1 cleaves only provitamin A carotenoids (except lycopene) specifically at the 15-15′ bond to yield retinal (9) is only consistent with the latter's biological importance. Thus, the existence of a carotenoid 9′,10′-oxygenase in vertebrates is interesting. Current literature suggests that the primary function of BCO2 in mice is to prevent oxidative stress from accumulation of carotenoids in the mitochondria (6), and so far, a

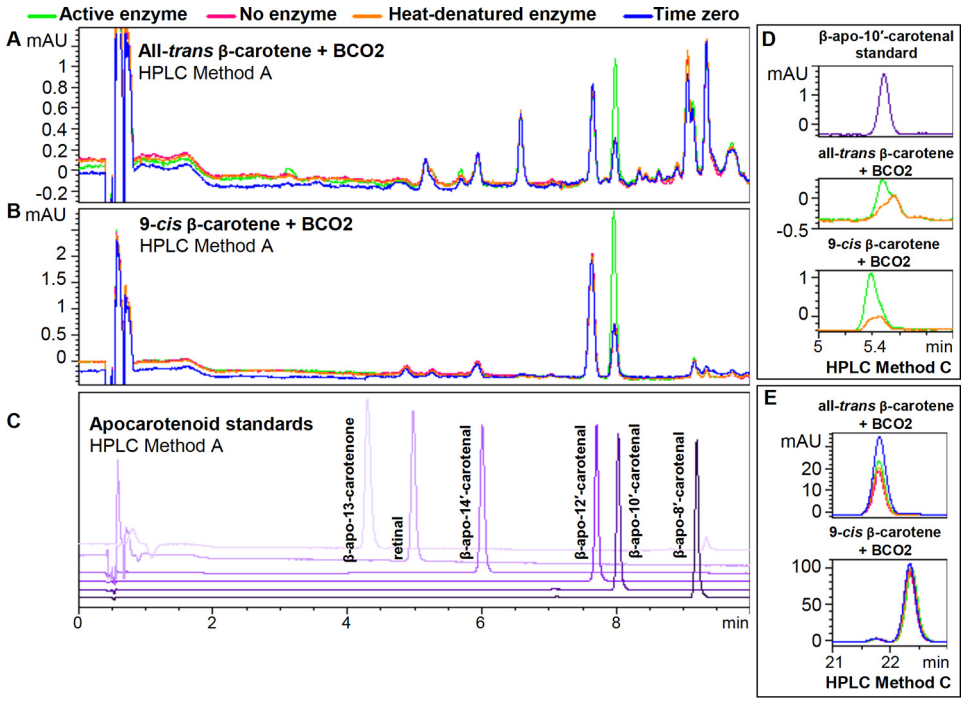

FIGURE 5. **Purified recombinant chicken BCO2 cleaves all-*trans*- and 9-*cis*-β-carotene.** The reaction was conducted for 2 h at 37 °C using 10 μg of BCO2/200-μl reaction and 20 μM substrate as described under "Experimental Procedures." Chromatograms were taken at 453 nm. Time 0, no enzyme, and heat-denatured enzyme controls were used. The *green* trace is the chromatogram for the reaction with the active enzyme; *pink*, no enzyme; *orange*, heat-denatured enzyme; *blue*, time 0 control. Standard compounds are shown in different shades of *purple*. Shown are the chromatograms for the reaction of BCO2 with all-*trans*-β-carotene (*A*) and 9-*cis*-β-carotene (*B*) and standard apocarotenoids (*C*) using HPLC Method A as described under "Experimental Procedures." D, using HPLC Method C (as described under "Experimental Procedures"), the retention time of the cleavage product of all-*trans*-β-carotene (*middle panel*) is identical to that of standard β-apo-10′-carotenal (*top panel*), whereas the cleavage product of 9-*cis*-β-carotene elutes earlier (*bottom panel*). *E*, there was no isomerization of the all-*trans*-β-carotene substrate (*top panel*) and 9-*cis*-β-carotene substrate (*bottom panel*) during the reaction as monitored by HPLC Method C. *mAU*, milli-absorbance units.

specific biological activity for β-apo-10′-carotenoids in vertebrates has not been identified (20) apart from their provitamin A activity (9, 21, 22).

The inactivity of human BCO2 in the *in vitro* assay systems tested can be explained by two possibilities. One is that it really is inactive or has very low activity, which can explain why full-length xanthophylls (lutein, 3′-epilutein, and zeaxanthin) are found in the human macula (10) despite BCO2 being highly expressed in the human retinal epithelium (12). Li *et al.* (13) noted four residues in human BCO2 (GKAA, positions 169–172; Fig. 1) that are not present in murine BCO2. However, expression of human BCO2 with the GKAA deletion in *E. coli* engineered to synthesize zeaxanthin failed to decrease the yellow color of the cells (an indication of carotenoid cleavage) unlike murine BCO2. In contrast, insertion of the GKAA into murine BCO2 resulted in retention of the yellow color. The GKAA sequence is also absent in all isoforms of chicken BCO2 (Fig. 1). However, the GKAA sequence is present in macaque BCO2, and activity was observed for heterologously expressed macaque BCO2 with an N terminus truncation (14).

The other possibility is that because it is associated with the inner mitochondrial membrane, as demonstrated by Palczewski *et al.* (23), it becomes misfolded during lysis or is missing the interactions with the membrane or membrane proteins necessary for activity. A similar phenomenon is observed for the related enzyme RPE65, which is also membrane-associated (24) and inactive when purified, but the activity is restored when it is reassociated with liposomes (25). In the study by Palczewski *et al.* (23), β-apo-10′-carotenal is produced when human BCO2 is expressed in *E. coli* engineered to synthesize β-carotene, possibly because BCO2 is still properly folded within the cell and/or has the necessary interactions with membranes and/or other proteins. Thus, the possibility that human BCO2 is active *in vivo* still cannot be completely ruled out.

As mentioned in our results, the recombinant chicken BCO2 we used differs from the chicken BCO2 isoform *x2* in the N terminus, which is where the mitochondrial targeting sequence, if any, would be located (26). This may have been a happy accident that made the protein more amenable to purification. However, Li *et al.* (13) replaced the N-terminal 197 amino acids of human BCO2 with the N-terminal 150 amino acids of murine BCO2, but this did not result in an observable cleavage of zeaxanthin in their cell-based assay. They also substituted a range of amino acid residues of human BCO2 with the corresponding residues of mouse BCO2, but this failed to confer detectable activity. Palczewski *et al.* (23) expressed human BCO2 with the N-terminal mitochondrial targeting sequence truncated at different lengths in β-carotene-producing *E. coli* and observed β-apo-10′-carotenal production with all variants of the enzyme. However, they also did not observe activity in cell-free systems (14).

Our results show that, with the exception of β-cryptoxanthin, chicken BCO2 cleaves carotenoids specifically at the 9-10 or 9′-10′ position to yield an apo-10′-carotenal. The ability of chicken BCO2 to cleave β-cryptoxanthin at the 7′-8′ double bond to produce 3-hydroxy-β-apo-8′-carotenal is possibly due

FIGURE 6. **Structures of the 9-10 and 9′-10′ cleavage of α-carotene, β-cryptoxanthin, zeaxanthin, and lutein.** An additional product resulting from 7′-8′ cleavage was observed for β-cryptoxanthin, and the structure is also shown here.

to the asymmetry of the molecule, causing a minor, alternative binding mode with BCO2.

As of the time of writing, there are no available crystal structures of BCO1 and BCO2. The only carotenoid oxygenase crystal structures available are those for an apocarotenoid 15,15′-oxygenase (27) and a 9-*cis*-epoxycarotenoid 11,12-oxygenase (28). Based on these crystal structures, the carotenoid oxygenases discriminate between substrates by the size of the hydrophobic substrate tunnel and the interactions of certain hydrophobic and aromatic residues (for a review, see Sui *et al.* (29)). Our experiments with BCO1 show that hydroxylation of the ring in β-cryptoxanthin results in a lower K_m compared with β-carotene and total loss of activity when the two rings are hydroxylated as in zeaxanthin (9). This suggests that a hydroxyl group may form unfavorable interactions with the hydrophobic substrate tunnel of BCO1 or that it is simply an issue of size; *i.e.* the 3-hydroxy-β-ionone ring is too large to pass through the substrate tunnel. The ability of BCO2 to cleave both carotenoids with and without 3-hydroxyl groups on the ionone rings, as shown by this study and others (6, 7), suggests that the substrate tunnel of BCO2 is larger than that of BCO1 and/or that the 3-hydroxyl groups do not form unfavorable interactions with the hydrophobic substrate tunnel.

BCO2 clearly catalyzes the oxidative cleavage of 9-*cis*-β-carotene (Fig. 5) and produces *mostly* 9-*cis*-β-apo-10′-carotenal (as discussed under "Results," the production of the all-*trans* product cannot be completely ruled out). This is not surprising because if the enzyme were to produce all-*trans*-β-apo-10′-carotenal, the kinked *cis* 9-10 end of 9-*cis*-β-carotene would have to enter the substrate tunnel. The size of the substrate tunnel may not allow for this, and thus BCO2 is regioselective (or even regiospecific) for the *trans* 9′-10′ end of 9-*cis*-β-carotene.

The large difference in the product peak areas obtained from the hydrocarbon carotenoids (β-carotene and α-carotene) compared with the hydroxylated carotenoids (β-cryptoxanthin, lutein, and zeaxanthin) (Figs. 5 and 7) suggests that hydroxylated carotenoids are the preferred substrates of the enzyme. It is worth noting that, at the lowest concentration tested for the β-cryptoxanthin substrate-velocity plot (7.5 μM; Fig. 9), the sum of the specific activities for β-apo-10′-carotenal and 3-hydroxy-β-apo-10′-carotenal production is 12× greater than that at the highest concentration tested for β-carotene (5 μM; Fig. 3*C*). Furthermore, at saturating β-cryptoxanthin, the sum of the specific activities for β-apo-10′-carotenal and 3-hydroxy-β-apo-10′-carotenal production is 33× greater than the calculated V_{max} for β-carotene. Kinetic data obtained using lysates from ferret BCO2-expressing Sf9 cells also suggest that lutein and zeaxanthin, which both contain 3- and 3′-hydroxyl groups, are better substrates than β-cryptoxanthin, which contains only one 3-hydroxyl group (7). Our semiquantitative results, at this point, also support this, although determination of kinetic parameters is necessary to make this conclusive. Similar to the issue with β-cryptoxanthin noted under "Results,"

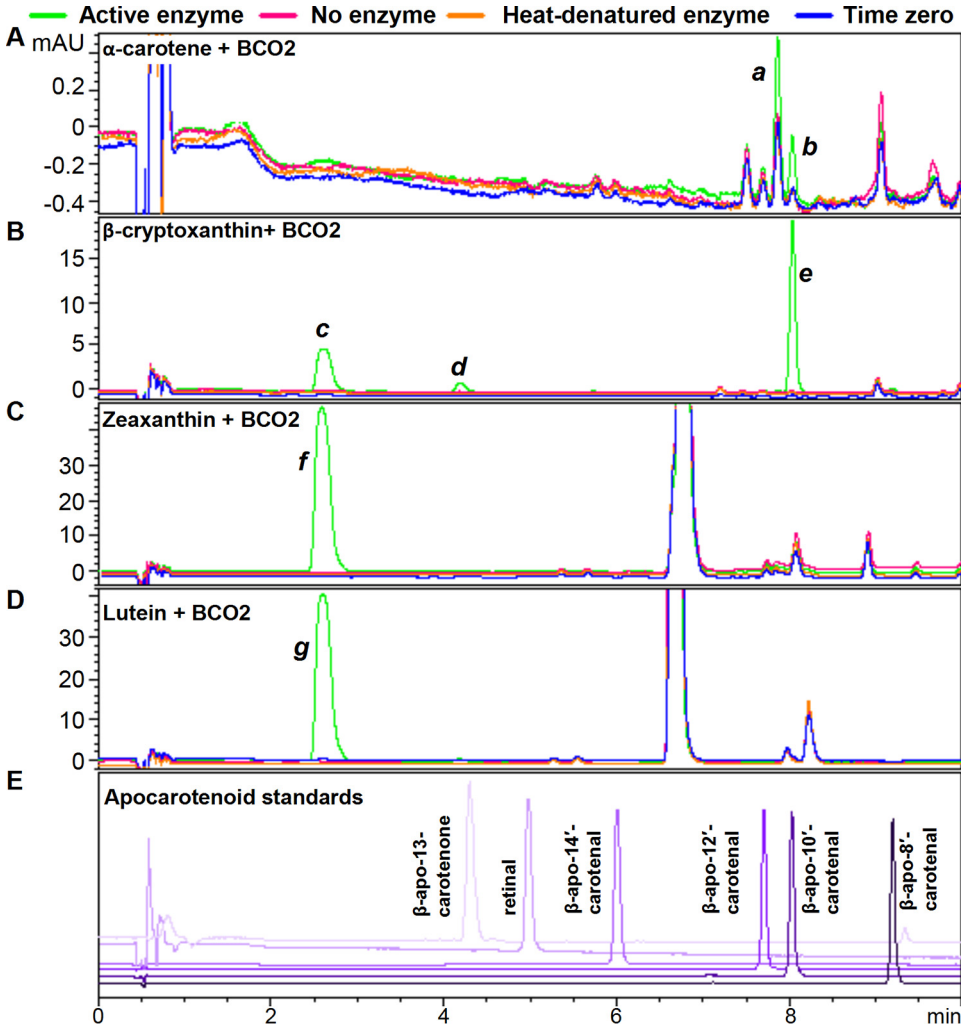

FIGURE 7. **Purified recombinant chicken BCO2 cleaves α-carotene, β-cryptoxanthin, zeaxanthin, and lutein.** The reactions were conducted for 2 h at 37 °C using 10 μg of BCO2/200-μl reaction and 20 μM substrate as described under "Experimental Procedures." Chromatograms were taken at 453 nm. Time 0, no enzyme, and heat-denatured enzyme controls were used. The *green* trace is the chromatogram for the reaction with the active enzyme; *pink*, no enzyme; *orange*, heat-denatured enzyme; *blue*, time 0 control. Standard compounds are shown in different shades of *purple*. Shown are the chromatograms for the reaction of BCO2 with α-carotene (*A*), β-cryptoxanthin (*B*), zeaxanthin (*C*), and lutein (*D*), and standard apocarotenoids (*E*) using HPLC Method A (as described under "Experimental Procedures"). Identified peaks are as follows: *a*, α-apo-10′-carotenal; *b* and *e*, β-apo-10′-carotenal; *c*, 3-hydroxy-β-apo-10′-carotenal; *d*, 3-hydroxy-β-apo-8′-carotenal; *f*, 3-hydroxy-β-apo-10′-carotenal; *g*, 3-hydroxy-β-apo-10′-carotenal and 3-hydroxy-α-apo-10′-carotenal. *mAU*, milli-absorbance units.

asymmetrical full-length carotenoids that are cleaved at two sites presumably have two binding modes and thus two K_m values. This should be taken into consideration when comparing K_m values with symmetrical substrates such as β-carotene.

The differences in peak areas of the product peaks from the asymmetrical carotenoid substrates (α-carotene, β-cryptoxanthin, and lutein) (Figs. 7 and 10) suggest that the enzyme displays an apparent regioselectivity. As mentioned previously, we do not have the standards for quantification of cleavage products except for β-apo-10′-carotenal, and thus we cannot conclude with absolute certainty that the small differences in peak areas of the product peaks of α-carotene (Fig. 7*A*) and lutein (Fig. 10) are due to true regioselectivity or the differences in extinction coefficients of the compounds as well as other factors that contribute to instrument response. With β-cryptoxanthin, the difference between the β-apo-10′-carotenal and 3-hydroxy-β-apo-10′-carotenal product peaks (Fig. 7*B*) is larger. The difference in the extinction coefficients of these two compounds is not expected to be very large (18), and thus it is likely (and not surprising) that the enzyme really does display regioselectivity with β-cryptoxanthin.

Unlike murine BCO2 (6), chicken BCO2 cannot perform a second cleavage on β-apo-10′-carotenal to yield rosafluene dialdehyde. If galloxanthin (3-hydroxy-β-apo-10′-carotenol) is an important carotenoid in avian vision and is indeed generated via BCO2 cleavage of zeaxanthin or lutein (Fig. 6), then it makes functional sense that chicken BCO2 does not cleave apo-10′-carotenals. If the function of BCO2 in mice is to degrade excess carotenoids, then it also makes functional sense that it can cleave full-length carotenoids twice, producing smaller molecules that are easier to clear from the circulation.

Chicken BCO2 has no activity with all-*trans*-lycopene, which is in agreement with the report on ferret BCO2 (30). This is also consistent with the preference of BCO2 for substrates that contain a 3-hydroxy-β-ionone ring. Ferret BCO2, however, is able to cleave *cis* isomers of lycopene (30). Ferrets accumulate *cis*-

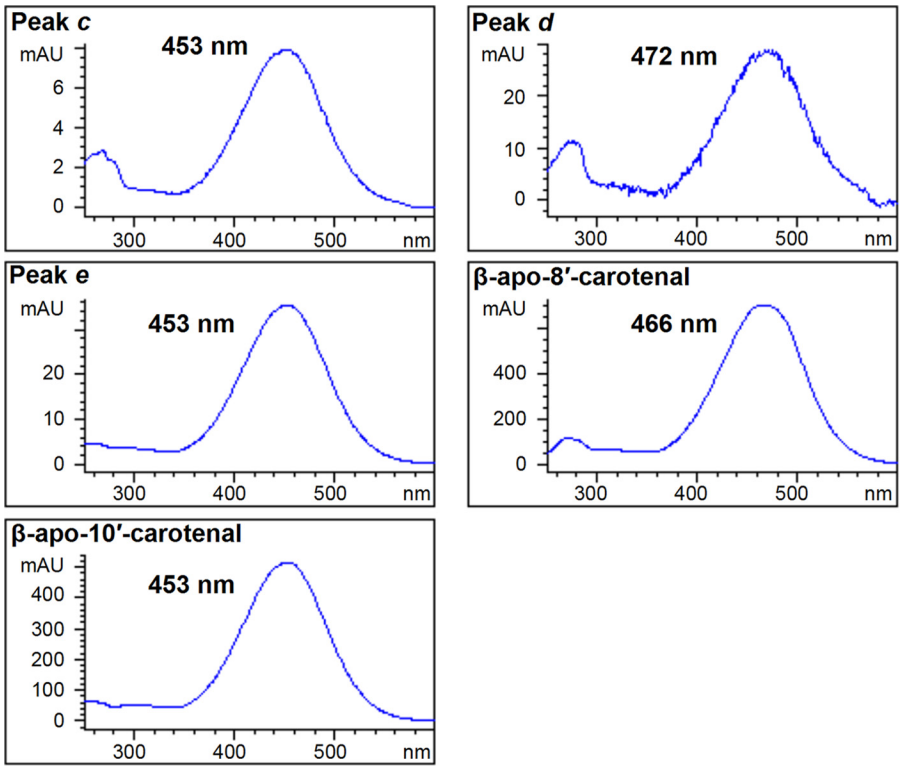

FIGURE 8. **UV-visible spectra of β-apo-8′-carotenal, β-apo-10′-carotenal, and their putative 3-hydroxylated counterparts produced from the reaction of chicken BCO2 with β-cryptoxanthin.** The λ_{max} is shown for each spectrum. The peak *numbers* correspond to the chromatogram peaks identified in Fig. 7*B*. Peak *e* has the same UV-visible spectra and retention time as standard β-apo-10′-carotenal. Peak *c* elutes much earlier but has the same λ_{max} as β-apo-10′-carotenal. This is consistent with its LC-MS identification as 3-hydroxy-β-apo-10′-carotenal by LC-MS. Peak *d* elutes after peak *c* but much earlier than peak *e*, and the UV-visible spectrum is similar to that of standard β-apo-8′-carotenal. This is consistent with its LC-MS identification as 3-hydroxy-β-apo-8′-carotenal by LC-MS. *mAU*, milli-absorbance units.

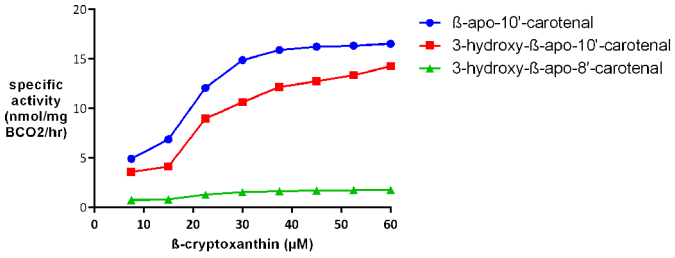

FIGURE 9. **Substrate velocity plot for chicken BCO2 with β-cryptoxanthin at 37 °C.** A plot of reaction velocity as a function of β-cryptoxanthin concentration using 1 μg of BCO2/200-μl reaction and a 30-min reaction time is shown. The amounts of 3-hydroxy-β-apo-10′-carotenal and 3-hydroxy-β-apo-8′-carotenal were estimated using β-apo-10′-carotenal and β-apo-8′-carotenal as standards. Each data point represents the average of duplicate experiments.

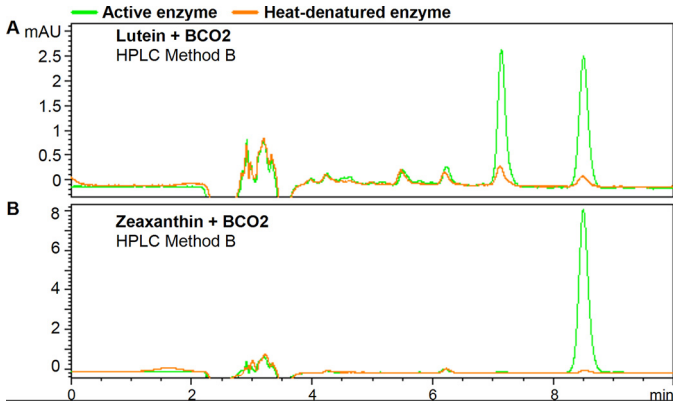

FIGURE 10. **Purified recombinant chicken BCO2 cleaves lutein to yield 3-hydroxy-β-apo-10′-carotenal and 3-hydroxy-α-apo-10′-carotenal.** The reactions are as described in Fig. 6, but the chromatography was done with HPLC Method B (as described under "Experimental Procedures"). Shown are the chromatograms for the reaction of BCO2 with lutein (*A*) and zeaxanthin (*B*). BCO2 cleavage of lutein yields 3-hydroxy-β-apo-10′-carotenal and 3-hydroxy-α-apo-10′-carotenal, whereas that of zeaxanthin yields only 3-hydroxy-β-apo-10′-carotenal. *mAU*, milli-absorbance units.

lycopene isomers when supplemented with all-*trans*-lycopene (30). Thus, the preference of ferret BCO2 for the latter is consistent with its proposed role of preventing excess accumulation of carotenoids. Similarly, the majority of lycopene in human fluids and tissues are *cis* isomers (31, 32), and it will not be surprising if human BCO2 can also catalyze their oxidative cleavage. The acid, alcohol, and aldehyde forms of the 9′-10′ cleavage product of lycopene have shown biological activity in cell culture, inducing retinoic acid receptor β mRNA levels and phase II enzymes at the mRNA and protein levels (33).

Chicken BCO2 also does not have activity with the other β-apocarotenals in the series (β-apo-8′-carotenal, β-apo-12′-carotenal, and β-apo-14′-carotenal). Again, this is consistent with the importance of the 3-hydroxy-β-ionone ring for BCO2 cleavage. β-carotene, with two β-ionone rings, is a relatively poor substrate, and it is not surprising that the β-apocarotenals, with only one β-ionone ring per molecule, are altogether inactive.

It is interesting that the substrates that are inactive with BCO2 (all-*trans*-lycopene and β-apocarotenals) are substrates for BCO1 (Fig. 11). With the β-apocarotenals, this

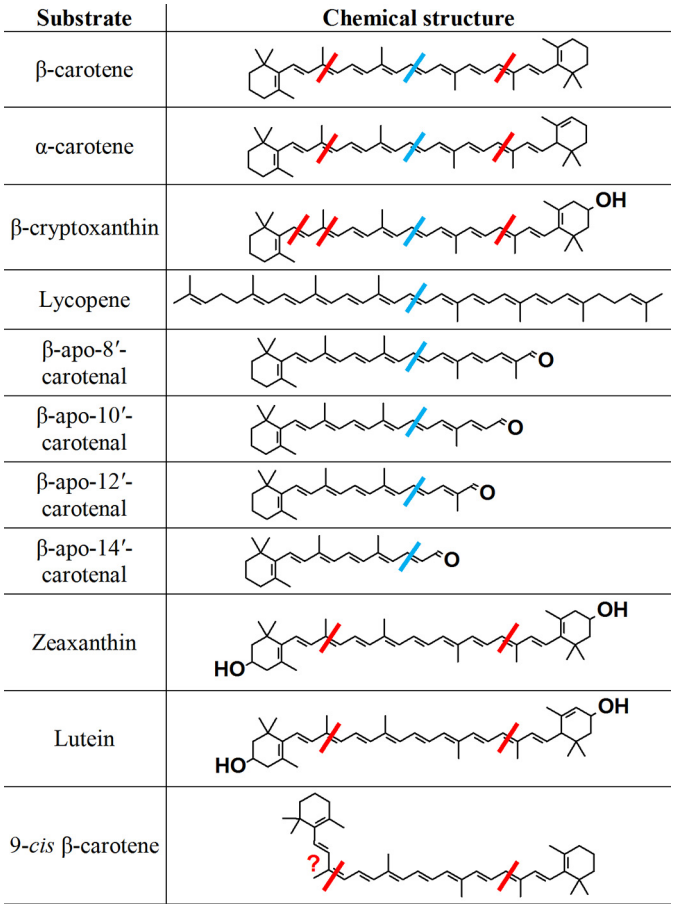

FIGURE 11. **Structures of the substrates tested with purified recombinant chicken BCO2 and human BCO1 (9).** The red bars represent the cleavages observed with BCO2, and the blue bars, BCO1.

difference in substrate specificities of the two enzymes is apparently to favor the production of retinal, which is not surprising given the latter's biological importance. It is tempting to apply the same logic to all-*trans*-lycopene, which would imply that there is potentially some importance in favoring the production of acycloretinal. However, acycloretinoids have been shown to have weak activity compared with retinoids (34–36), and they have not been detected in biological systems (33).

In summary, our results show that chicken BCO2 has broader substrate specificity than BCO1, consistent with its proposed function of preventing oxidative stress brought about by carotenoid accumulation in the mitochondria. It cleaves only full-length carotenoids with ionone rings, and the hydroxylated carotenoids are cleaved to a greater extent than their hydrocarbon counterparts under the conditions tested. Furthermore, the enzyme displays regioselectivity with asymmetrical substrates.

Author Contributions—E. H. H. conceived and coordinated the study and cowrote the paper with C. d. S. C. d. S., J. S., and Y. Y. prepared the enzyme and designed, conducted, and analyzed the enzymology experiments. S. N. and R. W. C. synthesized compounds. K. M. R., S. J. S., and C. d. S. designed and conducted the LC-MS experiments. All authors reviewed the results and approved the final version of the manuscript.

Acknowledgments—We thank Drs. Matthew B. Toomey and Joseph Corbo of Washington University at St. Louis for the pET-28a-chicken BCO2 plasmid, Morgan Cichon for the lycopene standard, and Sara Thomas for assistance with HPLC separation of the cleavage products of lutein and zeaxanthin.

References

1. Jin, M., Li, S., Moghrabi, W. N., Sun, H., and Travis, G. H. (2005) Rpe65 is the retinoid isomerase in bovine retinal pigment epithelium. *Cell* **122,** 449–459
2. Hamel, C. P., Tsilou, E., Pfeffer, B. A., Hooks, J. J., Detrick, B., and Redmond, T. M. (1993) Molecular cloning and expression of RPE65, a novel retinal pigment epithelium-specific microsomal protein that is post-transcriptionally regulated *in vitro*. *J. Biol. Chem.* **268,** 15751–15757
3. Redmond, T. M., Poliakov, E., Yu, S., Tsai, J. Y., Lu, Z., and Gentleman, S. (2005) Mutation of key residues of RPE65 abolishes its enzymatic role as isomerohydrolase in the visual cycle. *Proc. Natl. Acad. Sci. U.S.A.* **102,** 13658–13663
4. Moiseyev, G., Chen, Y., Takahashi, Y., Wu, B. X., and Ma, J. X. (2005) RPE65 is the isomerohydrolase in the retinoid visual cycle. *Proc. Natl. Acad. Sci. U.S.A.* **102,** 12413–12418
5. Lyubarsky, A. L., Savchenko, A. B., Morocco, S. B., Daniele, L. L., Redmond, T. M., and Pugh, E. N., Jr. (2005) Mole quantity of RPE65 and its productivity in the generation of 11-*cis*-retinal from retinyl esters in the living mouse eye. *Biochemistry* **44,** 9880–9888
6. Amengual, J., Lobo, G. P., Golczak, M., Li, H. N., Klimova, T., Hoppel, C. L., Wyss, A., Palczewski, K., and von Lintig, J. (2011) A mitochondrial enzyme degrades carotenoids and protects against oxidative stress. *FASEB J.* **25,** 948–959
7. Mein, J. R., Dolnikowski, G. G., Ernst, H., Russell, R. M., and Wang, X. D. (2011) Enzymatic formation of apo-carotenoids from the xanthophyll carotenoids lutein, zeaxanthin and β-cryptoxanthin by ferret carotene-9′,10′-monooxygenase. *Arch. Biochem. Biophys.* **506,** 109–121
8. Amengual, J., Widjaja-Adhi, M. A., Rodriguez-Santiago, S., Hessel, S., Golczak, M., Palczewski, K., and von Lintig, J. (2013) Two carotenoid oxygenases contribute to mammalian provitamin A metabolism. *J. Biol. Chem.* **288,** 34081–34096
9. dela Seña, C., Narayanasamy, S., Riedl, K. M., Curley, R. W., Jr., Schwartz, S. J., and Harrison, E. H. (2013) Substrate specificity of purified recombinant human β-carotene 15,15′-oxygenase (BCO1). *J. Biol. Chem.* **288,** 37094–37103
10. Toomey, M. B., and McGraw, K. J. (2007) Modified saponification and HPLC methods for analyzing carotenoids from the retina of quail: implications for its use as a nonprimate model species. *Invest. Ophthalmol. Vis. Sci.* **48,** 3976–3982
11. Lobo, G. P., Amengual, J., Li, H. N., Golczak, M., Bonet, M. L., Palczewski, K., and von Lintig, J. (2010) β,β-Carotene decreases peroxisome proliferator receptor γ activity and reduces lipid storage capacity of adipocytes in a β,β-carotene oxygenase 1-dependent manner. *J. Biol. Chem.* **285,** 27891–27899
12. Lindqvist, A., He, Y. G., and Andersson, S. (2005) Cell type-specific expression of β-carotene 9′,10′-monooxygenase in human tissues. *J. Histochem. Cytochem.* **53,** 1403–1412
13. Li, B., Vachali, P. P., Gorusupudi, A., Shen, Z., Sharifzadeh, H., Besch, B. M., Nelson, K., Horvath, M. M., Frederick, J. M., Baehr, W., and Bernstein, P. S. (2014) Inactivity of human β,β-carotene-9′,10′-dioxygenase (BCO2) underlies retinal accumulation of the human macular carotenoid pigment. *Proc. Natl. Acad. Sci. U.S.A.* **111,** 10173–10178
14. Babino, D., Palczewski, G., Widjaja-Adhi, M. A., Kiser, P. D., Golczak, M., and von Lintig, J. (2015) Characterization of the role of β-carotene 9,10-dioxygenase in macular pigment metabolism. *J. Biol. Chem.* **290,** 24844–24857
15. Eroglu, A., Hruszkewycz, D. P., dela Sena, C., Narayanasamy, S., Riedl, K. M., Kopec, R. E., Schwartz, S. J., Curley, R. W., Jr., and Harrison, E. H. (2012) Naturally occurring eccentric cleavage products of provitamin A

β-carotene function as antagonists of retinoic acid receptors. *J. Biol. Chem.* **287,** 15886–15895
16. Kim, Y. S., Yeom, S. J., and Oh, D. K. (2011) Production of β-apo-10′-carotenal from β-carotene by human β-carotene-9′,10′-oxygenase expressed in *E. coli*. *Biotechnol. Lett.* **33,** 1195–1200
17. Poliakov, E., Gentleman, S., Cunningham, F. X., Jr., Miller-Ihli, N. J., and Redmond, T. M. (2005) Key role of conserved histidines in recombinant mouse β-carotene 15,15′-monooxygenase-1 activity. *J. Biol. Chem.* **280,** 29217–29223
18. Britton, G. (1995) UV/visible spectroscopy, in *Carotenoids* (Britton, G., Liaaen-Jensen, S., and Pfander, H., eds) Vol. 1B, pp. 13–62, Birkhäuser Verlag, Basel, Switzerland
19. Walter, M. H., Floss, D. S., and Strack, D. (2010) Apocarotenoids: hormones, mycorrhizal metabolites and aroma volatiles. *Planta* **232,** 1–17
20. Eroglu, A., and Harrison, E. H. (2013) Carotenoid metabolism in mammals, including man: formation, occurrence, and function of apocarotenoids. *J. Lipid Res.* **54,** 1719–1730
21. Grolier, P., Duszka, C., Borel, P., Alexandre-Gouabau, M. C., and Azais-Braesco, V. (1997) *In vitro* and *in vivo* inhibition of β-carotene dioxygenase activity by canthaxanthin in rat intestine. *Arch. Biochem. Biophys.* **348,** 233–238
22. Kim, Y. S., and Oh, D. K. (2009) Substrate specificity of a recombinant chicken β-carotene 15,15′-monooxygenase that converts β-carotene into retinal. *Biotechnol. Lett.* **31,** 403–408
23. Palczewski, G., Amengual, J., Hoppel, C. L., and von Lintig, J. (2014) Evidence for compartmentalization of mammalian carotenoid metabolism. *FASEB J.* **28,** 4457–4469
24. Kiser, P. D., and Palczewski, K. (2010) Membrane-binding and enzymatic properties of RPE65. *Prog. Retin. Eye Res.* **29,** 428–442
25. Nikolaeva, O., Takahashi, Y., Moiseyev, G., and Ma, J. X. (2009) Purified RPE65 shows isomerohydrolase activity after reassociation with a phospholipid membrane. *FEBS J.* **276,** 3020–3030
26. Gakh, O., Cavadini, P., and Isaya, G. (2002) Mitochondrial processing peptidases. *Biochim. Biophys. Acta* **1592,** 63–77
27. Kloer, D. P., Ruch, S., Al-Babili, S., Beyer, P., and Schulz, G. E. (2005) The structure of a retinal-forming carotenoid oxygenase. *Science* **308,** 267–269
28. Messing, S. A., Gabelli, S. B., Echeverria, I., Vogel, J. T., Guan, J. C., Tan, B. C., Klee, H. J., McCarty, D. R., and Amzel, L. M. (2010) Structural insights into maize Viviparous14, a key enzyme in the biosynthesis of the phytohormone abscisic acid. *Plant Cell* **22,** 2970–2980
29. Sui, X., Kiser, P. D., von Lintig, J., and Palczewski, K. (2013) Structural basis of carotenoid cleavage: from bacteria to mammals. *Arch. Biochem. Biophys.* **539,** 203–213
30. Hu, K. Q., Liu, C., Ernst, H., Krinsky, N. I., Russell, R. M., and Wang, X. D. (2006) The biochemical characterization of ferret carotene-9′,10′-monooxygenase catalyzing cleavage of carotenoids *in vitro* and in *vivo*. *J. Biol. Chem.* **281,** 19327–19338
31. Richelle, M., Sanchez, B., Tavazzi, I., Lambelet, P., Bortlik, K., and Williamson, G. (2010) Lycopene isomerisation takes place within enterocytes during absorption in human subjects. *Br. J. Nutr.* **103,** 1800–1807
32. Krinsky, N. I., Russett, M. D., Handelman, G. J., and Snodderly, D. M. (1990) Structural and geometrical isomers of carotenoids in human plasma. *J. Nutr.* **120,** 1654–1662
33. Wang, X.-D. (2009) Biological activities of carotenoid metabolites, in *Carotenoids* (Britton, G., Liaaen-Jensen, S., and Pfander, H., eds) Vol. 5, pp. 383–408, Birkhäuser Verlag, Basel, Switzerland
34. Kotake-Nara, E., Kim, S. J., Kobori, M., Miyashita, K., and Nagao, A. (2002) Acyclo-retinoic acid induces apoptosis in human prostate cancer cells. *Anticancer Res.* **22,** 689–695
35. Ben-Dor, A., Nahum, A., Danilenko, M., Giat, Y., Stahl, W., Martin, H. D., Emmerich, T., Noy, N., Levy, J., and Sharoni, Y. (2001) Effects of acyclo-retinoic acid and lycopene on activation of the retinoic acid receptor and proliferation of mammary cancer cells. *Arch. Biochem. Biophys.* **391,** 295–302
36. Stahl, W., von Laar, J., Martin, H. D., Emmerich, T., and Sies, H. (2000) Stimulation of gap junctional communication: comparison of acyclo-retinoic acid and lycopene. *Arch. Biochem. Biophys.* **373,** 271–274
37. Larkin, M. A., Blackshields, G., Brown, N. P., Chenna, R., McGettigan, P. A., McWilliam, H., Valentin, F., Wallace, I. M., Wilm, A., Lopez, R., Thompson, J. D., Gibson, T. J., and Higgins, D. G. (2007) Clustal W and Clustal X version 2.0. *Bioinformatics* **23,** 2947–2948
38. Robert, X., and Gouet, P. (2014) Deciphering key features in protein structures with the new ENDscript server. *Nucleic Acids Res.* **42,** W320–W324